Influence of graphene coating on speckle-pattern rotation of light in gyrotropic optical fiber

Dmitry A. Kuzmin,[1,*] Igor V. Bychkov,[1] and Vladimir G. Shavrov[2]

[1]*Chelyabinsk State University, 129 Br. Kashirinykh Street, Chelyabinsk 454001, Russian Federation*

[2]*Kotelnikov Institute of Radio-Engineering and Electronics of RAS, 11/7 Mokhovaya Street, Moscow 125009, Russian Federation*

Corresponding author: kuzminda89@gmail.com

In the present work, change in speckle-pattern of linearly polarized light passed through graphene-covered optical fiber placed in external magnetic field is investigated. The possibility of magnetic speckle-pattern rotation suppression and inverse speckle-pattern rotation effect is shown. This effect can be controlled by a chemical potential of graphene layer, which can be changed easily by a gate voltage, for example. For quartz optical fiber at wavelength 0.633 μm, core diameter 9 μm, and fiber length 5 cm, an inverse rotation value of 17° is reached at chemical potential of graphene layer about 1 eV and magnetic field strength 30 kOe. Results of the work may be useful for different magneto-optics, opto-electronics, and photonics applications. © 2015 Optical Society of America

OCIS codes: (060.2280) Fiber design and fabrication; (060.2310) Fiber optics; (060.2370) Fiber optics sensors; (120.0280) Remote sensing and sensors; (130.0250) Optoelectronics; (130.2790) Guided waves.

http://dx.doi.org/10.1364/OL.40.000890

It is well known that when light is traveling into the gyrotropic medium, its polarization plane rotates due to Faraday effect. In [1], the possibility of observable speckle-pattern (radiation distribution at cross-section of the fiber) rotation of light passed through the gyrotropic optical fiber placed in longitudinal magnetic field has been predicted. It has been shown as well that modes corresponding to the meridional rays are mainly responsible for the rotation of the speckle-pattern. Then such an effect has been observed experimentally for linearly polarized light traveling through low-mode quartz fiber placed in longitudinal magnetic field [2]. Some theoretical explanations of the effect based on peculiarity theory approach have been made in works [3,4]. Method of detecting magnetic field variation employing the rotation of the speckle-pattern has been proposed and implemented experimentally [5].

Nowadays, great attention of researchers is attracted by graphene—two-dimensional honey-comb-like carbon lattice [6–10]. Graphene layer can support both TE- and TM-polarized highly localized surface plasmon polaritons [11–15]. Multilayer graphene-based structures have a number of interesting properties, including waveguide ones [16–18]. Structures based on graphene and gyrotropic materials have some features as well [19,20].

This present work is devoted to investigation of how coating of fiber core by graphene layer will affect speckle-pattern rotation. Investigation showed the possibility of inverse speckle-pattern rotation of linearly polarized light in such a fiber. This effect can be controlled be chemical potential of graphene layer. Investigated features may have both fundamental interest (interaction of light polarization with its trajectory) and various practical applications (determining the properties of graphene by the angle of the speckle-pattern rotation, for photonics and optoelectronics devices, etc.).

We will consider a round gyrotropic fiber with radius and a, length l, and step-like refractive index profile, wherein graphene layer is placed between core and shell of the fiber (see. Fig. 1). To solve the problem, one has to solve Maxwell's equations with material equations and boundary conditions at $r = a$:

$$(\mathbf{E}_c - \mathbf{E}_{sh}) \times \mathbf{n} = 0; \qquad (\mathbf{H}_c - \mathbf{H}_{sh}) \times \mathbf{n} = 4\pi\mathbf{j}/c. \quad (1)$$

Lowerscripts "c" and "sh" denote the fields in core and shell of the fiber, respectively, $\mathbf{n}$ is a normal vector, directed from core to shell of the fiber, $\mathbf{j}$ is a surface current density in graphene layer, and c is speed of light in vacuum. For optical frequencies, we may assume that both core and shell of the fiber are nonmagnetic (magnetic susceptibility is scalar $\mu = 1$). Electric permittivity tensor $\hat{\varepsilon}$ for gyrotropic medium has a form

$$\hat{\varepsilon}_{sh}^{c} = \begin{pmatrix} \varepsilon_{xx} & \varepsilon_{xy} & 0 \\ \varepsilon_{yx} & \varepsilon_{yy} & 0 \\ 0 & 0 & \varepsilon_{zz} \end{pmatrix}, \qquad \varepsilon_{xx} = \varepsilon_{yy} = \varepsilon_{sh}^{c}, \qquad \varepsilon_{zz} = \varepsilon_{\parallel sh}^{c},$$

$$\varepsilon_{xy} = -\varepsilon_{yx} = i\varepsilon_{sh}^{ac}. \quad (2)$$

Let us assume that fields $\mathbf{E}$ and $\mathbf{H}$ have a harmonical time dependence $\sim\exp(i\omega t)$, where ω is the circular frequency. In such a case, for traveling along z-axis, wave components of the electromagnetic field may be represented in cylindrical system of coordinates [21,22]

$$\mathbf{E}, \mathbf{H} = \sum_{m=-\infty}^{\infty} \sum_{n=0}^{N_m} \mathbf{E}, \mathbf{H}_{m,n}(r) \exp(im\varphi - i\beta_{m,n}z). \quad (3)$$

Here, $\mathbf{E}_{m,n}(r)$ and $\mathbf{H}_{m,n}(r)$ are the radial distributions of electric and magnetic fields of mode with number m, and traveling along z-axis with propagation constant $\beta_{m,n}$. For core of the fiber such distribution is a superposition of Bessel's functions $J_m(\kappa_{i,m,n}r)$, $i = 1,2$, and its derivatives. For shell of the fiber, one has to use McDonald's functions $K_m(\xi_{i,m,n}r)$, $i = 1,2$ instead of Bessel's ones. $\kappa_{i,m,n}$ and $\xi_{i,m,n}$ have a meaning of the transverse propagation constants. These values may be expressed through the $\beta_{m,n}$:

$$\kappa_{1,2}^2 = \frac{1}{2}[k_0^2(\varepsilon_{\|c} + \varepsilon_{\perp c}) - \beta^2(1 + \varepsilon_{\|c}\varepsilon_c^{-1})]$$

$$\pm \left\{ \frac{1}{4}\left[k_0^2(\varepsilon_{\|c} - \varepsilon_{\perp c}) - \beta^2\left(\frac{\varepsilon_{\|c}}{\varepsilon_c} - 1\right)\right]^2 \right.$$

$$\left. + k_0^2\beta^2\varepsilon_{\|c}\left(\frac{\varepsilon_{ac}}{\varepsilon_c}\right)^2 \right\}^{1/2}$$

$$\xi_{1,2}^2 = \frac{1}{2}[\beta^2(1 + \varepsilon_{\|sh}\varepsilon_{sh}^{-1}) - k_0^2(\varepsilon_{\|sh} + \varepsilon_{\perp sh})]$$

$$\pm \left\{ \frac{1}{4}\left[k_0^2(\varepsilon_{\|sh} - \varepsilon_{sh}) - \beta^2\left(\frac{\varepsilon_{\|sh}}{\varepsilon_{sh}} - 1\right)\right]^2 \right.$$

$$\left. + k_0^2\beta^2\varepsilon_{\|sh}\left(\frac{\varepsilon_{ash}}{\varepsilon_{sh}}\right)^2 \right\}^{1/2}. \tag{4}$$

In Eq. (4), the following notations have been introduced: $\varepsilon_{\perp} = \varepsilon - \varepsilon_a^2/\varepsilon$, $k_0 = \omega/c$ is a wavenumber of electromagnetic wave in vacuum. Solutions number of this equation is N_m. Putting electromagnetic field in form Eq. (3) with taking into account Eq. (4) into the boundary conditions Eq. (1), we will obtain characteristic equation for mode with number m. Solving this equation, we can determine the propagation constants $\beta_{m,n}$.

For numerical calculations we will use parameters for quartz fiber [2]: core radius $a = 4.5$ μm, core refractive index $n_c = (\varepsilon_c)^{1/2} = 1.47$, shell refractive index $n_{sh} = (\varepsilon_{sh})^{1/2} = 1.466$, let us assume that $\varepsilon_{\|} = \varepsilon$. Verde constants of core and shell will be considered as equals. They define an antisymmetric part of the electric permittivity $\varepsilon_a = VH_0\lambda\varepsilon^{1/2}/\pi$. For quartz fiber, $V = 4.1 \cdot 10^{-10}$ rad/(Gs μm). Wavelength of light $\lambda = 0.633$ μm (the wavelength of the He–Ne laser). The fiber with core radius 4.5 μm works in few-mode regime at wavelength 0.633 μm [2–5]. Increasing the fiber diameter leads to increase the number of modes. As will be seen below, this is no crucial for the effect.

Characteristic equation has a form:

$$\det\begin{pmatrix} a_{11} & a_{12} & -a_{13} & -a_{14} \\ a_{21} - \frac{4\pi}{c}\sigma a_{31} & a_{22} - \frac{4\pi}{c}\sigma a_{32} & -a_{23} & -a_{24} \\ a_{31} & a_{32} & -a_{33} & -a_{34} \\ a_{41} + \frac{4\pi}{c}\sigma a_{11} & a_{42} + \frac{4\pi}{c}\sigma a_{12} & -a_{43} & -a_{44} \end{pmatrix} = 0,$$

$$a_{1j} = -\frac{\varepsilon_a\kappa_j^2}{\varepsilon}J_m(\kappa_j a), \qquad a_{2j} = -i\frac{\kappa_j^2}{k_0\beta}J_m(\kappa_j a),$$

$$a_{3j} = T_j\kappa_j J'_m(\kappa_j a) + \varepsilon_a\frac{m}{a}\left(k_0^2 - \frac{\kappa_j^2}{\varepsilon}\right)J_m(\kappa_j a),$$

$$a_{4j} = k_0\varepsilon_a\kappa_j J'_m(\kappa_j a) + \frac{T_j}{k_0}\frac{m}{a}J_m(\kappa_j a),$$

$$j = 1,2, \qquad T_{1,2} = k_0^2\varepsilon - \beta^2 - \kappa_{1,2}^2. \tag{5}$$

Expressions for a_{ij}, $j = 3,4$ may be obtained by change in (5) $\kappa_i \to \xi_i$, $\kappa_i^2 \to -\xi_i^2$, $J_m(\kappa_i a) \to K_m(\xi_i a)$. Equation (5) may be solved numerically by iterative Newton method. So, we will have propagation constants $\beta_{m,n}$, $\kappa_{i,m,n}$, and $\xi_{i,m,n}$. Putting this constants in Eq. (3), we will get the field distribution, and the problem will be solved.
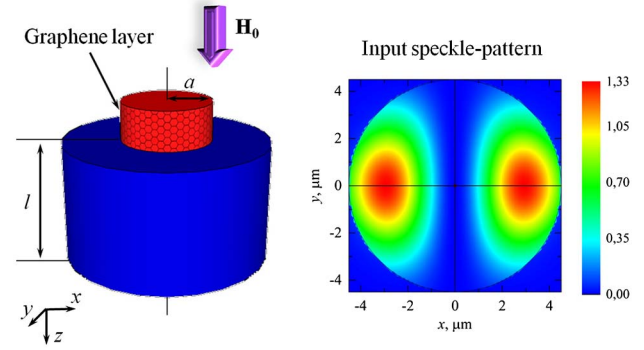

Fig. 1. Scheme of graphene-coated optical fiber and input speckle-pattern distribution.

Let us consider an input electromagnetic field

$$E_{0x} \sim \exp\left[-\frac{(r - a/2)^2}{a^2/4}\right]\cos(\varphi)\exp(i\omega t - ik_0 z),$$

$$E_{0y} = 0. \tag{6}$$

For such input distribution, only four modes with $m = \pm 2$, $n = 1$; $m = 0$, $n = 1,2$ may be exited. Speckle-pattern $I_x = E_x E_x^*$ of input distribution is shown on Fig. 1.

Conductivity of graphene layer may be calculated by the formulas [23]:

$$\sigma(\omega) = ie^2\pi^{-1}\hbar^{-2}(\omega - 2i\Gamma)$$

$$\times \left[\begin{array}{l}(\omega - 2i\Gamma)^{-2}\int_0^\infty \zeta\left(\frac{\partial f(\zeta)}{\partial\zeta} - \frac{\partial f(-\zeta)}{\partial\zeta}\right)\mathrm{d}\zeta - \\ \int_0^\infty \frac{f(-\zeta) - f(\zeta)}{(\omega - 2i\Gamma)^2 - 4(\zeta/\hbar)^2}\mathrm{d}\zeta\end{array}\right]. \tag{7}$$

Here, $\hbar$ is the Plank's constant, $f(\zeta) = [\exp((\zeta - \mu_{ch})/k_B T) + 1]^{-1}$ is the Fermi–Dirac distribution, μ_{ch} is the chemical potential of graphene layer, k_B is the Boltzmann's constant, T is the temperature, and Γ is the electron's collisions rate. Chemical potential may be changed, for example, by doping or gate voltage. It is well known that there is some critical value of the chemical potential, when real part of the graphene conductivity sharply decreases and imaginary part becomes positive (see Fig. 2). Such a feature has a place when photon energy $\hbar\omega$ is close to the interband absorption threshold $\sim 2\mu_{ch}$. When imaginary part of graphene conductivity is positive, graphene layer can support both TE- and TM-polarized plasmon polaritons [11] [indeed, authors [11] showed, that plasmon polaritons of both polarizations may exist at *negative* imaginary part of conductivity, but they used time dependence of the fields $\sim \exp(-i\omega t)$, when we use $\sim \exp(i\omega t)$].

Nonzero real part of conductivity becomes a reason of energy dissipation when electromagnetic wave is guided by the fiber (propagation constants $\beta_{m,n}$ are complex). Analytical calculations show that characteristic equation has a term with multiplier $m\sigma\varepsilon_a$ [multipliers $\sigma a_{31,2}$ in (5)]. So, when sign of the conductivity is changed, relation between phase speeds for modes with different m signs is changed as well. Calculations show that at negative
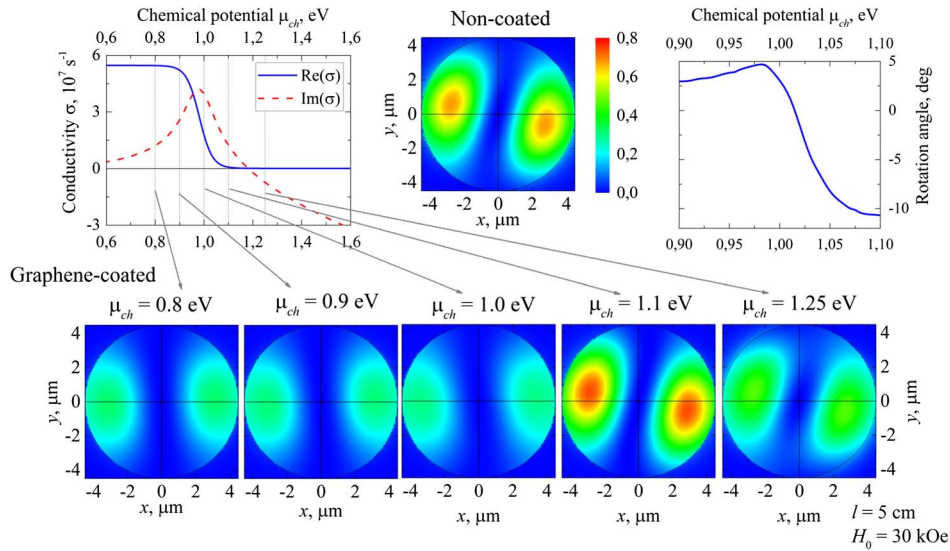
Fig. 2. Chemical potential dependence of real and imaginary parts of graphene conductivity, speckle-pattern $I_x(x, y)$ for fiber length 5 cm, magnetic field value $H_0 = 30$ kOe, and different values of chemical potential of graphene layer, dependence of the rotation angle from the chemical potential value near the interband threshold.

imaginary part of conductivity (like usually for metals and semiconductors), phase speed of modes with negative m is greater than speed of modes with $m > 0$. The same situation has a place for noncoated fiber. This is the reason of the clockwise speckle-pattern rotation (looking along wave guiding direction). Change in sign of imaginary part of conductivity leads to change of graphene contribution to mode's phase speeds (modes with $m < 0$ are slowing down, with $m > 0$ are speeding up). This decreases speckle-pattern rotation, and at some conditions, it may cause an inverse speckle-pattern rotation (counterclockwise speckle-pattern rotation). One can also note that for single-mode fiber (only one mode with $m = 0$ may propagate in the fiber), speckle-patter rotation cannot be observed. So, few-mode regime is essential for the effect observation.

Chemical potential dependence of real and imaginary parts of graphene, speckle-pattern $I_x(x, y)$ for fiber length 5 cm, magnetic field value $H_0 = 30$ kOe, and different values of chemical potential of graphene layer are shown on Fig. 2. Figure 2 shows speckle-pattern for non-coated fiber as well. One can see that graphene coating may compensate the rotation of the speckle-pattern typical for a gyrotropic fiber without graphene. When imaginary part of conductivity reaches a maximum [$\mu_{ch} \approx 1$ eV, see Fig. 2], speckle-pattern rotates counterclockwise (rotation angle is about 4.7° counterclockwise; for noncoated fiber rotation angle is about 12.5° clockwise). Total effect of graphene coating is a counterclockwise rotation on angle about 17° for fiber length 5 cm, magnetic field 30 kOe, and chemical potential of graphene layer 0.98 eV. The maximum of intensity is changed as well. This fact may be explained by superposition of Faraday and Cotton–Mouton effects.

Note that values of chemical potential we used for calculation ($\mu_{ch} \sim 1$ eV) may be easily reachable in experiments [6–8]. Nowadays, characteristic length of the graphene layers that can be produced is about some microns. Our calculations show that for some evident

effect, coated fiber of some centimeters length is needed. However, it is not essential to coat the fiber core by a single continuous graphene layer for the effect observation. It is necessary to have very thin layer of material with a positive imaginary part of conductivity. Several graphene layers can be used for such purposes. In addition, we used material parameters of the quartz fiber from experiment [2]. Choice of material for the fiber with a larger Verdet constant may enhance the effects observed, and hence reduce the required length of the fiber and magnetic field strength. For example, the Verdet constant of rare-earth-doped YIG commonly used in the magnetooptics is about 3–5 orders of magnitude larger than values we used in our calculations [24–28]. Figure 3 shows comparison of the speckle-pattern rotation effect
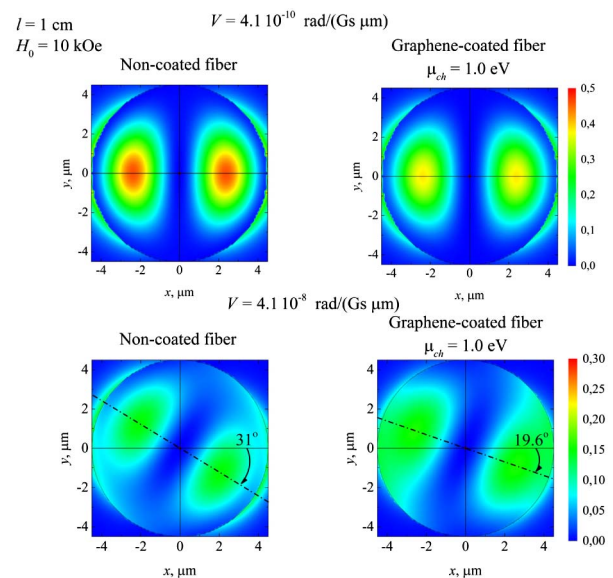

Fig. 3. Comparison of the speckle-pattern rotation effect for fiber length 1 cm, magnetic field strength 10 kOe, and different Verdet constants.

for fiber length 1 cm, magnetic field strength 10 kOe, and different Verdet constants. One can see that for quartz fiber Verdet constant $V = 4.1 \cdot 10^{-10}$ rad/(Gs μm), there is not any evident speckle-pattern rotation for both non coated and graphene-coated fibers. For Verdet constant two times greater $V = 4.1 \cdot 10^{-8}$ rad/(Gs μm), there is clockwise speckle-pattern rotation for noncoated fiber on about 31°. Graphene coating has an effect of inverse speckle-pattern rotation on about 19.6° clockwise. So, graphene coating leads to counterclockwise rotation on angle about 11°.

In conclusion, note that external magnetic field have different effects for different modes of propagating waves. In the present Letter, we investigated only modes with $m = 0, \pm 2$. For each m, there are N_m different waves with propagation constants $\beta_{m,n}$. Electromagnetic field at fixed fiber length is a superposition of all such waves, so speckle-pattern will strictly depend on the fiber length. All these features have to be investigated more deeply. Results of such investigation will be published elsewhere soon.

Finally, our study showed the possibility of linearly polarized light speckle-pattern manipulation by both magnetic field and chemical potential of graphene changing (for example, by a gate voltage). This possibility may be used for light manipulation in various opto-electronic and photonics applications. By the other hand, one can measure coating layer properties by speckle-pattern rotation angle, or suppress magnetic speckle-pattern rotation, when it is necessary.

References

1. N. B. Baranova and B. Y. Zel'dovich, J. Exp. Theor. Phys. Lett. **59**, 681 (1994).
2. M. Y. Darsht, I. V. Zhirgalova, B. Y. Zel'dovich, and N. D. Kundikova, J. Exp. Theor. Phys. Lett. **59**, 763 (1994).
3. L. I. Ardasheva, M. O. Sadykova, N. R. Sadykov, V. E. Chernyakov, V. V. Anikeev, M. V. Bol'shakov, A. I. Valeev, V. S. Zinatulin, and N. D. Kundikova, J. Opt. Technol. **69**, 451 (2002).
4. L. I. Ardasheva, N. D. Kundikova, M. O. Sadykova, N. R. Sadykov, and V. E. Chernyakov, Opt. Spectrosc. **95**, 645 (2003).
5. M. V. Bolshakov, A. V. Ershov, and N. D. Kundikova, Opt. Spectrosc. **110**, 624 (2011).
6. R. R. Nair, P. Blake, A. N. Grigorenko, K. S. Novoselov, T. J. Booth, T. Stauber, N. M. R. Peres, and A. K. Geim, Science **320**, 1308 (2008).
7. F. Bonaccorso, Z. Sun, T. Hasan, and A. C. Ferrari, Nat. Photonics **4**, 611 (2010).
8. Q. Bao and K. P. Loh, ACS Nano **6**, 3677 (2012).
9. L. A. Falkovsky, Phys. Usp. **55**, 1140 (2012).
10. P. He, L. Li, J. Yu, W. Huang, Y. C. Yen, L. J. Lee, and A. Y. Yi, Opt. Lett. **38**, 2625 (2013).
11. S. A. Mikhailov and K. Ziegler, Phys. Rev. Lett. **99**, 016803 (2007).
12. Yu. V. Bludov, M. I. Vasilevskiy, and N. M. R. Peres, Eur. Phys. Lett. **92**, 68001 (2010).
13. F. H. L. Koppens, D. E. Chang, and F. J. G. de Abajo, Nano Lett. **11**, 3370 (2011).
14. A. Vakil and N. Engheta, Science **332**, 1291 (2011).
15. B. E. Sernelius, Phys. Rev. B **85**, 195427 (2012).
16. I. V. Iorsh, I. S. Mukhin, I. V. Shadrivov, P. A. Belov, and Yu. S. Kivshar, Phys. Rev. B **87**, 075416 (2013).
17. D. Smirnova, P. Buslaev, I. Iorsh, I. V. Shadrivov, P. A. Belov, and Yu. S. Kivshar, Phys. Rev. B **89**, 245414 (2014).
18. H. Huang, B. Wang, H. Long, K. Wang, and P. Lu, Opt. Lett. **39**, 5957 (2014).
19. D. A. Kuzmin, I. V. Bychkov, and V. G. Shavrov, Photon. Nanostruct. Fundam. Appl. **12**, 473 (2014).
20. D. A. Kuzmin, I. V. Bychkov, and V. G. Shavrov, IEEE Trans. Magn. **50**, 1 (2014).
21. A. G. Gurevich and G. A. Melkov, *Magnetization Oscillations and Waves* (CRC Press, 1996).
22. A. A. Th. M. Van Trier, Appl. Sci. Res. B **3**, 305 (1953).
23. G. W. Hanson, J. Appl. Phys. **103**, 064302 (2008).
24. G. B. Scott and D. E. Lacklison, IEEE Trans. Mag. **12**(4), 292 (1976).
25. C. F. Buhrer, J. Appl. Phys. **41**, 1393 (1970).
26. V. J. Fratello, S. J. Licht, and C. D. Brandle, IEEE Trans. Mag. **32**(5), 4102 (1996).
27. S. Parchenko, A. Stupakiewicz, I. Yoshimine, T. Satoh, and A. Maziewski, Appl. Phys. Lett. **103**, 172402 (2013).
28. A. H. Rose, M. N. Deeter, and G. W. Day, Opt. Lett. **18**, 1471 (1993).